

Steel and Composite Structures, Vol. 5, No. 6 (2005)

Technical Report

Numerical modelling and codification of imperfections for cold-formed steel members analysis

Dan Dubina†

*Department of Steel Structures and Structural Mechanics, Faculty of Civil Engineering,
"Politehnica" University of Timisoara, I. Curea 1, Timisoara, 300224, Romania*

Viorel Ungureanu‡

Laboratory of Steel Structures, Romanian Academy, Timisoara Branch, M. Viteazul 24, 300223, Romania

Jacques Rondal‡‡

*Department of Mechanics of Materials and Structures, University of Liège,
Chemin des Chevreuils 1, B-4000, Liège, Belgium*

(Received December 8, 2004, Accepted May 17, 2005)

Abstract. Buckling and post-buckling of cold-formed steel members are rather difficult to predict due to material and geometrical non-linearity. However, numerical techniques have reached a level of maturity such that many are now successfully undertaking ultimate strength analysis of cold-formed steel members. In numerical non-linear analysis, both geometrical and material imperfections, have to be estimated and properly used. They must be codified in terms of shape and magnitude. The presented paper represents a state-of-art report, including relevant results obtained by the authors and collected from literature, on that problem.

Key words: thin-walled cold-formed members; material and geometrical imperfections; numerical modelling; codification.

1. Introduction

Due to the local and distortional instability phenomena, and their coupling with overall buckling modes, the post-critical behaviour of thin-walled cold-formed steel members is highly non-linear, being very difficult to predict using analytical methods. Numerical non-linear analysis is successfully used to simulate the real behaviour of cold-formed steel sections and to evaluate their effective properties. Two general reports presented by Rasmussen (1996) and Sridharan (2000) during the 2nd and 3rd International Conferences on Coupled Instabilities in Metal Structures, reviewed numerical simulations and computational models used for coupled instability problems. Also, Bakker and Peköz (2003) summarised the basic principles of FEM analysis of thin-walled members. However, the first condition to succeed in

†Professor, Corresponding author, E-mail: ddubina@ceft.utt.ro

‡Senior Researcher

‡‡Professor

numerical simulations is not the accurate theoretical formulation nor highly performance solution techniques, available by commercial software like ANSYS, ABAQUS, NASTRAN and others, but the knowledge of the initial state of member subjected to analysis. Particularly, in case of cold-formed steel sections, accurate characterisation of geometrical imperfections and residual stresses is largely unavailable, and the distribution of the yield strength along the perimeter of the cross-section is non-uniform due to cold-forming process. A good knowledge of these fundamental quantities is absolutely necessary for reliable completion of advanced numerical simulation of cold-formed steel members, and the presented paper attempts to show how it can be managed.

2. Mechanical properties of cold-formed steel members

2.1. Influence of cold-forming

Thin-walled steel sections are fabricated by means of cold-rolling of coils or press-braking of plates made by carbon steel. However, for these members, frequently used in modern steel constructions, the initial σ - ϵ relation of the steel is considerably changed by the cold-straining due to the manufacturing processes. Fig. 1(a) shows the modification of the σ - ϵ diagram when a carbon steel specimen is first strained beyond the yield plateau and then unloaded. For modern steel the strain aging effect is now very rare, or at least limited. Therefore, only the cold-forming effect has to be considered in the computation and on this purpose the apparent σ - ϵ diagram (see Fig. 1(b)) can be used.

Due to the forming process strain-hardening can vary considerably along the cross-section as shown in Table 1 and Fig. 2.

Karren (1967) and Karren and Winter (1967) have proposed the following equation for the corner yield strength:

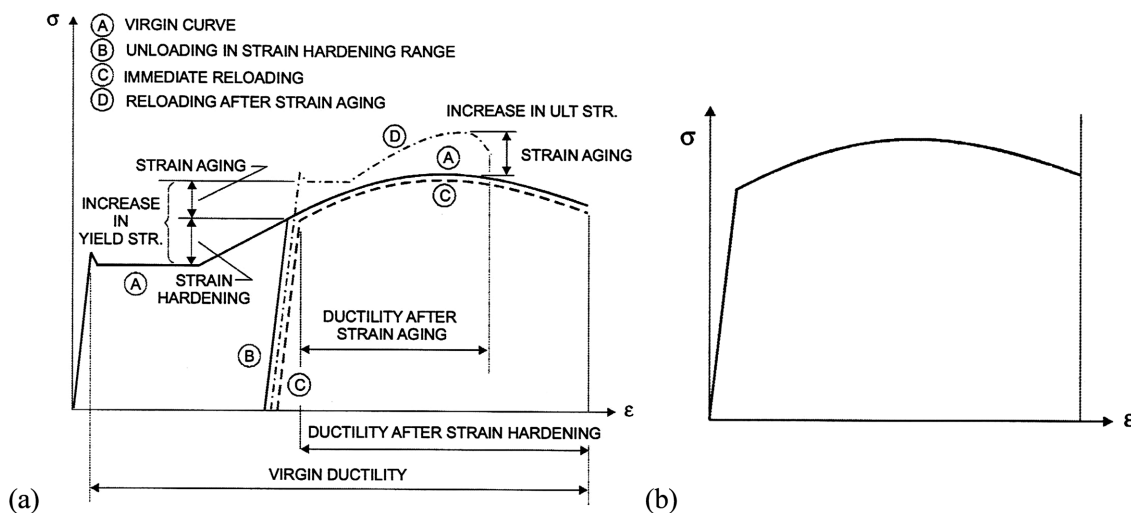


Fig. 1 Effects of cold straining and strain aging on σ - ϵ characteristics of carbon steel: (a) Global σ - ϵ diagram; (b) Apparent σ - ϵ diagram for a cold-formed member

Table 1 Influence of manufacturing process on the basic strengths of hot and cold-formed profiles (Rondal 2005)

Forming process		Cold rolling	Press braking
Yield strength (f_y)	Corner	high	high
	Flat faces	moderate	--
Ultimate strength (f_u)	Corner	high	high
	Flat faces	moderate	--

$$f_{yc} = \frac{k \cdot g}{(r/t)^h} \quad (1)$$

with $g = 0.945 - 1.315 \cdot q$ (2)

$$h = 0.803 \cdot q \quad (3)$$

where t is the thickness of the sheet, r is the inside bend radius, k and q are the parameters of the hardening law which are given by:

$$k = 2.80 \cdot f_u - 1.55 \cdot f_{yb} \quad (4)$$

$$q = 0.225 \cdot \frac{f_u}{f_{yb}} - 0.120 \quad (5)$$

where f_u is the virgin ultimate strength and f_{yb} the virgin yield strength of the sheet.

With regard to the full-section properties, the average tensile yield strength may be approximated by using a weighted average as follows (Karren and Winter 1967):

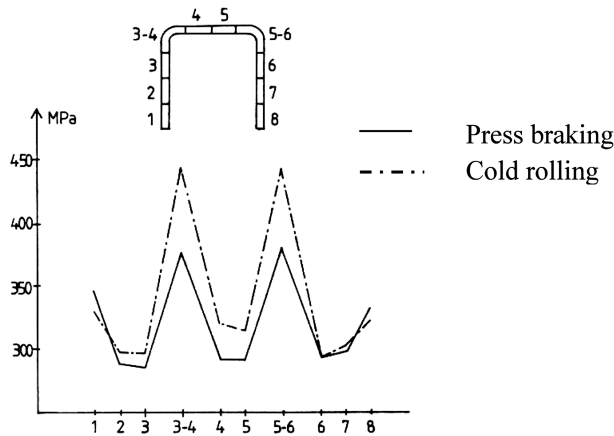


Fig. 2 Influence of manufacturing process on yield strength (Batista 1986)

$$f_{ya} = A_c \cdot f_{yc} + (1 + A_c) \cdot f_{yb} \quad (6)$$

where A_c is the ratio of corner area to total cross-sectional area.

Eurocode 3-Part 1.3 gives the following formula to evaluate the average yield strength, f_{ya} , of the full section. This formula is, in fact, a modification of Eq. (6) where a zone closed to the corner is considered as fully plastified:

$$f_{ya} = f_{yb} + (C \cdot n \cdot t^2 / A_g) \cdot (f_u - f_{yb}) \quad (7)$$

where A_g is the gross cross sectional area and n is the number of 90° bends in the section, with an internal radius $r < 5t$. In this formula, $C=7$ for cold-rolling and $C=5$ for other methods of forming.

$$f_{ya} \leq 0.5 \cdot (f_{yb} + f_u) \quad (8)$$

or

$$f_{ya} \leq 1.25 \cdot f_{yb} \quad (9)$$

The average yield strength, f_{ya} , can be used in numerical analysis when a bilinear stress-strain model approximates the material behaviour. However, if test results are available, the input parameters for material model are needed to describe the stress-strain behaviour, directly obtained from tensile coupon tests from different portions of the member cross-section.

2.2. Material modelling

Material modelling represents one of the most important aspects of the FE simulation. If tests results are not available, an idealisation of the material model, that is elastic-plastic with strain hardening, can be conveniently approximated by Ramberg-Osgood or Powell equations. Using ANSYS, the ideally elastic-plastic material model can be implemented by means of bilinear isotropic plastic model (BISO), and Ramberg-Osgood model by means of multi-linear model (MISO).

In Table 2 and Fig. 3 are shown the numerical results obtained with ANSYS large-deformation elastic-plastic analysis using the two material models (Dubina *et al.* 1997). One can see that both characteristic values and the shape of load-deflection curves do not differ significantly in the models.

An important role plays the corner properties. Due to the manufacturing process the material exhibits significant strain hardening in corner regions of the cold-formed section. They are characterised by an yield strength much higher than in the flat zone, and simultaneously by a reduced ductility. In case of standard carbon steel, Eq. (1) can be used for corner's F.E. strips. For stainless steel, Gardner and Nethercot (2004) proposed a simple model which can be applied to all types of corners to predict $\sigma_{0.2,c}$ by knowing the ultimate strength of virgin material, $\sigma_{u,v}$, i.e., $\sigma_{0.2,c} = 0.85 \cdot \sigma_{u,v}$.

Table 2 Limit loads in kN

Specimen	Tests	ANSYS with bilinear material model		ANSYS with R-O model
		measured imperfections	equivalent imperfections	measured imperfections
L36P0280-	83.5	-	85.87	81.41
L36P0815+	67.9	70.5	72.08	69.8
L36P1315-	41.1	41.42	38.56	40.75

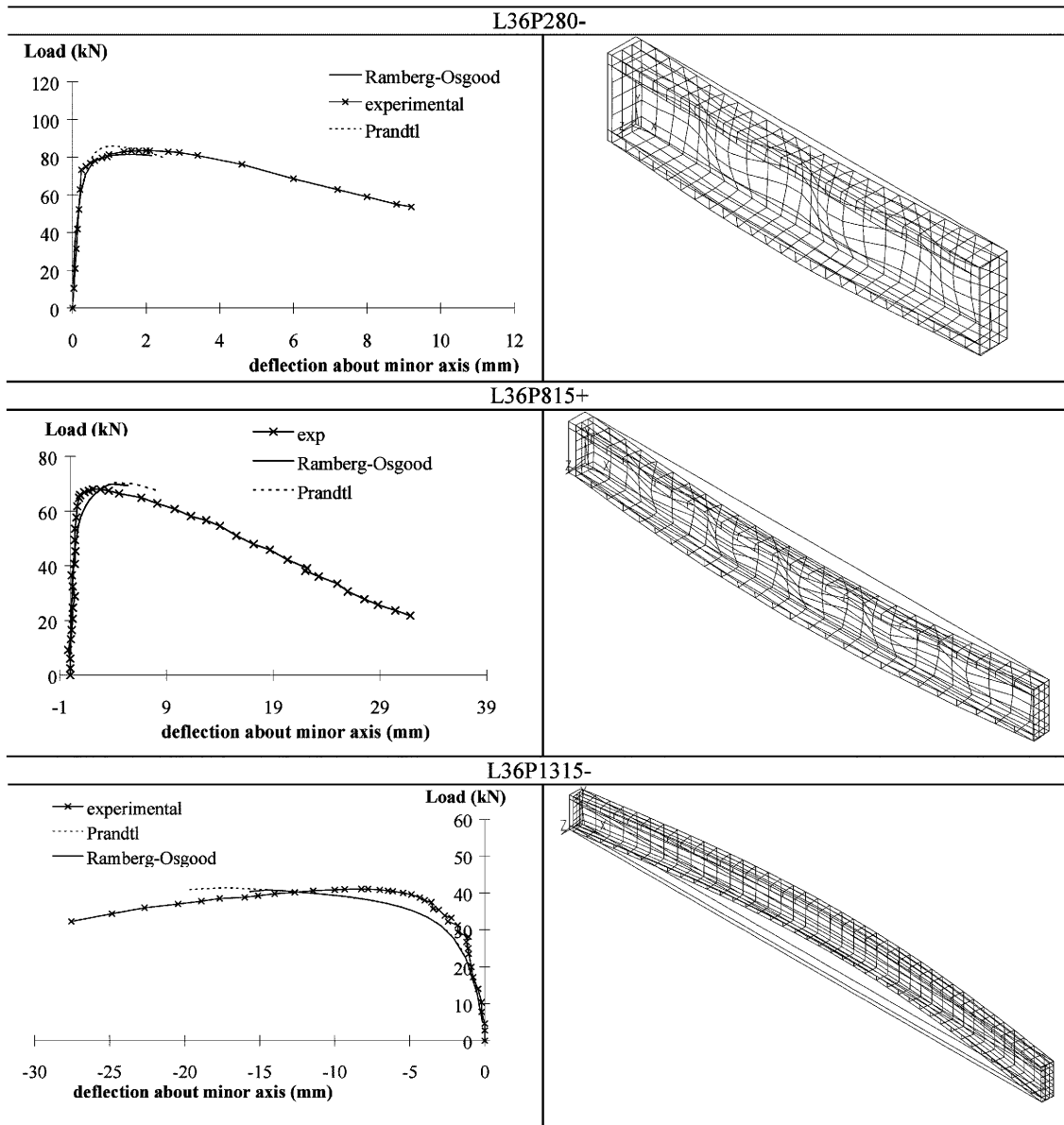


Fig. 3 Load versus mid-length deflection about minor axis and deformed shapes at the limit load

Also, Put, Pi and Trahair (1998) have proposed different material models for flat zones and the corners in the case of thin-wall cold-formed sections.

However, as Szabo (2004) showed in case of sections formed by press braking, which usually have small bent radius, the role of corner properties is insignificant. Fig. 4 displays the material curves used by Szabo in the analysis, on which he based his previous remark : *material 1* and *material 2* represent the alternative average σ - ε curves for the flat portions of the cross-section, while *material 3* represents the average σ - ε curve used for corners.

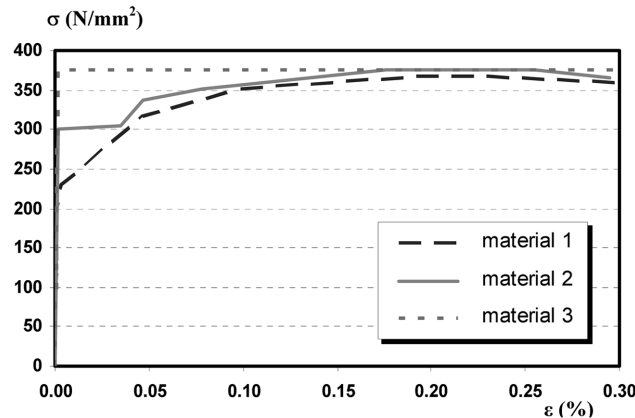


Fig. 4 Material models for numerical analysis

3. Geometrical imperfections

3.1. Shape of geometrical imperfections

When a geometrical non-linear analysis is performed, some kind of initial disturbances (e.g. imperfection) are necessary when the strength of the member is studied (Dubina 2000). In case of cold-formed steel sections, two kinds of imperfections are characteristic, i.e.,:

- geometrical imperfections, sectional and along the member;
- residual stress and change of yield strength due to cold forming effect.

When initial imperfections are used to invoke geometric non-linearity, the shape of imperfections can be determined with an eigenbuckling analysis and must be affine with the relevant local, sectional or overall buckling modes of the cross-section. Consequently, until now the geometrical imperfections are introduced in numerical models using equivalent sine shapes with half-wavelength corresponding to relevant instability modes. Rasmussen and Hancock (1988) and Schafer and Peköz (1998) proposed numerical models to generate automatically geometrical imperfection modes. Schafer *et al.* (1998) used the probabilistic analysis in order to evaluate the frequency and magnitude of imperfections.

Maximum measured imperfections can be conservatively used as amplitude in sine shape to predict by analysis lower bound strength (Rasmussen and Hancock 1988). While it is true that larger imperfections do not always mean lower strength, if the eigenmode shape used in the analysis does not characterise the most unfavourable imperfect shape of the member, generally the strength decreases as the magnitude of the imperfection increases. However, different shapes of local/sectional imperfections have different effect on the buckling strength of the member and, not always, the sine shape of geometrical imperfections represents the most relevant mode to be considered in the analysis. Since maximum imperfections are not periodic along the length, using the maximum amplitude of imperfection as for the buckled shape is rather conservative. Despite these drawbacks, the maximum imperfection approach is simple to apply and provides a reasonable criterion for a lower bound strength analysis. At this point, it is also useful to underline a conclusion by Bernard *et al.* (1999), who demonstrated statistically that a significant influence of geometrical imperfections exists in thin-walled members at short and medium wave-lengths, leading to reduction of the load carrying capacity. This means the sectional buckling modes, singly or coupled with overall ones, are mainly affected.

3.2. Codification of geometrical imperfections

Geometric imperfections refer to the deviation of member from the *perfect* or *nominal* geometry. Imperfections of cold-formed steel members include bowing, warping, and twisting as well as local deviations. Local deviations are characterised by dents and regular undulation on the plate. Collected data on geometric sectional imperfections are sorted by Schafer and Peköz (1998) in two categories (see Fig. 5): *type 1*, maximum local imperfection in a stiffened element (e.g. local buckling type imperfection), and *type 2*, maximum deviation from straightness for a lip stiffened or unstiffened flange (e.g. distortional type imperfection).

Based on statistical analysis of actual measurements, Schafer and Peköz (1998) proposed the following simple rules to apply when width/thickness (b/t) less than 200 for *type 1* imperfections, and (b/t) less than 100 for *type 2* imperfections, respectively. Thickness should be less than 3 mm. For *type 1* imperfections, a simple linear regression based on the plate width yields to the approximate expression

$$d_1 \approx 0.006 \cdot b \quad (10)$$

where b is width or depth of the web.

An alternative rule based on an exponential curve fits to the thickness (t)

$$d_1 \approx 6 \cdot t \cdot e^{-2t} \quad (d_1 \text{ and } t \text{ in mm}) \quad (11)$$

For *type 2* imperfections the maximum deviation from straight is approximately equal to the plate thickness:

$$d_2 \approx t \quad (12)$$

In what concern the overall sinusoidal imperfections (bar deflection), with the maximum amplitude of $1/1500$ times the member length, (L), which corresponds to statistical mean of imperfections of carbon steel columns, as suggested by Bjorhovde (1972), can be used, or more conservatively, $L/1000$, as proposed by ECCS Recommendation (1978).

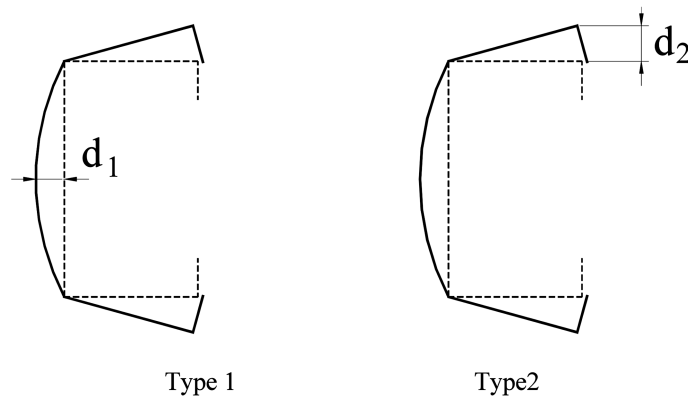


Fig. 5 Sectional imperfections

In case of lateral-torsional buckling of thin-walled beams, both initial deflection and initial twisting may be significant. On this purpose, the Australian Standard AS 4100 proposes recommendations for the initial deflection, (f_o) , and initial twist, (ϕ_o) , as follows:

$$1000 \cdot f_o / L = 1000 \cdot \phi_o \cdot (M_{cr} / N_{cr} L) = -1 \quad \text{for } \bar{\lambda}_{LT} \geq 0.6 \quad (13)$$

$$1000 \cdot f_o / L = 1000 \cdot \phi_o \cdot (M_{cr} / N_{cr} L) = -0.001 \quad \text{for } \bar{\lambda}_{LT} < 0.6 \quad (14)$$

where:

- N_{cr} = column elastic critical buckling (Euler) load about minor axis;
- M_{cr} = elastic critical moment for lateral-torsional buckling;
- $\bar{\lambda}_{LT}$ = flexural-torsional slenderness;
- L = length of the member.

3.3. Influence of the shape of sectional geometrical imperfections on the value of α -imperfection factor in European buckling curves

Based on numerical simulations Dubina and Ungureanu (2002) have systematically studied the influence of size and shape of sectional geometrical imperfections on the ultimate buckling strength of plain and lipped channel sections, both in compression and bending.

In the FE model used by authors, the maximum amplitudes proposed by Schafer and Pekoz (1998) for sectional imperfections of types 1 and 2 have been used. Different shapes of these imperfections, over the section and along the member, were considered into the elastic-plastic FEM simulations.

Tables 3 and 4 show the shape of sectional imperfections used for compression and bending members and the corresponding sectional ultimate buckling strengths.

With the sectional imperfections in Tables 3 and 4, the erosion of theoretical buckling strength, due to both the imperfections and interaction of sectional (e.g. either local or distortional) buckling mode with the overall one (either flexural or flexural-torsional), has been evaluated using the ECBL approach (Dubina 2001).

Assuming the two simple theoretical instability modes, which are coupling, the Euler bar theoretical instability mode, $\bar{N}_E = 1 / \lambda^2$, and the theoretical local-sectional instability one, $\bar{N}_{L,th}$, the erosion coefficient can be computed for four different imperfection cases (see Fig. 5), i.e.,

- $e_{c,th}$ = theoretical erosion due to coupling effect only;
- e_L = actual erosion due to local imperfections only;
- e_c = actual erosion due to coupling effect and global imperfection;
- e = actual total erosion due to both coupling and imperfections.

The following notations were used in Fig. 6:



















$\bar{N} = N / N_{pl}$, where N is the ultimate strength of the member; N_{pl} represents its corresponding full plastic strength;

$\bar{N}_{L,th} = N_{L,th} / N_{pl}$, with $N_{L,th}$, the ultimate theoretical short column strength;

$\bar{N}_L = N_L / N_{pl}$, N_L being the ultimate strength of imperfect stub column;

$\bar{\lambda} = \sqrt{N_L / N_{cr}}$, the reduced slenderness of the member.

Table 3 Shape of sectional (local or distortional) imperfections for compression members

Case No.	Plain Channel (U96x36x1.5)		N_{uL} (kN)	Lipped Channel (C96x36x12x1.5)		N_{uL} (kN)
L1		- local buckling PL1 (symmetric sine shape)	44.97		- local buckling LL1 (symmetric sine shape)	91.34
L2		- local buckling PL2 (asymmetric sine shape)	46.15		- local buckling LL2 (asymmetric sine shape)	91.81
L0		- local buckling PL3 (stub column without imperfections)	74.70		- local buckling LL3 (stub column without imperfections)	91.91
D1		- distortional buckling PD1 (the imperfection is constant on the whole length)	66.73		- distortional buckling LD1 (the imperfection is constant on the whole length)	80.33
D2		- distortional buckling PD2 (the imperfection is constant on whole length)	66.43		- distortional buckling LD2 (the imperfection is constant on whole length)	94.81
D3		- distortional buckling PD3 (symmetric sine shape)	41.04		- distortional buckling LD3 (symmetric sine shape)	76.63
D4		- distortional buckling PD4 (asymmetric sine shape)	39.29		- distortional buckling LD4 (asymmetric sine shape)	61.70
D5		- distortional buckling PD5 (the imperfection is constant on the whole length)	73.02		- distortional buckling LD5 (the imperfection is constant on the whole length)	74.52
D0		- distortional buckling PD6 (stub column without imperfections)	74.38		- distortional buckling LD6 (stub column without imperfections)	95.12

Maximum erosion of theoretical interactive buckling strength, e , is calculated in regard with the theoretical interaction point, $M(\bar{\lambda}_{int} = 1 / \sqrt{\bar{N}_{L,th}})$, and is defined as:

$$e = \bar{N}_{L,th} - \bar{N}(\bar{\lambda} = 1 / \sqrt{\bar{N}_L}) \quad (15)$$

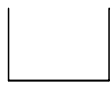
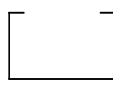







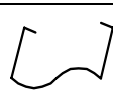

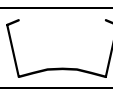
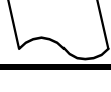

The total erosion can be associated with the α imperfection factor used in European buckling curves for members in compression, by means of ECBL formula:

$$\alpha = \frac{e^2}{1 - e} \cdot \frac{\sqrt{\bar{N}_L}}{1 - 0.2\sqrt{\bar{N}_L}} \quad (16)$$

In case of members in bending the α_{LT} formula given by ECBL approach is:

$$\alpha_{LT} = \frac{e_{LT}^2}{1 - e_{LT}} \cdot \frac{\sqrt{\bar{M}_L}}{1 - 0.4\sqrt{\bar{M}_L}} \quad (17)$$

Table 4 Shape of sectional (local or distortional) imperfections for bending members

Case No.	Plain Channel (U96×36×1.5)	M_{uL} (kNm)	Lipped Channel (C96×36×12×1.5)	M_{uL} (kNm)
D0		- distortional buckling PD1 (short beam without imperfections)		- distortional buckling LD6 (short beam without imperfections)
D1		- distortional buckling PD2 (the imperfection is constant on the whole length)		- distortional buckling LD1 (the imperfection is constant on the whole length)
D2		- distortional buckling PD3 (the imperfection is constant on whole length)		- distortional buckling LD2 (the imperfection is constant on whole length)
D3		- distortional buckling PD4 (the imperfection is constant on the whole length)		- distortional buckling LD5 (the imperfection is constant on the whole length)
D4		- distortional buckling PD5 (the imperfection is constant on the whole length)		- distortional buckling LD5 (the imperfection is constant on the whole length)
D5		- distortional buckling PD6 (symmetric sine shape)		- distortional buckling LD3 (symmetric sine shape)
D6		- distortional buckling PD7 (asymmetric sine shape)		- distortional buckling LD4 (asymmetric sine shape)

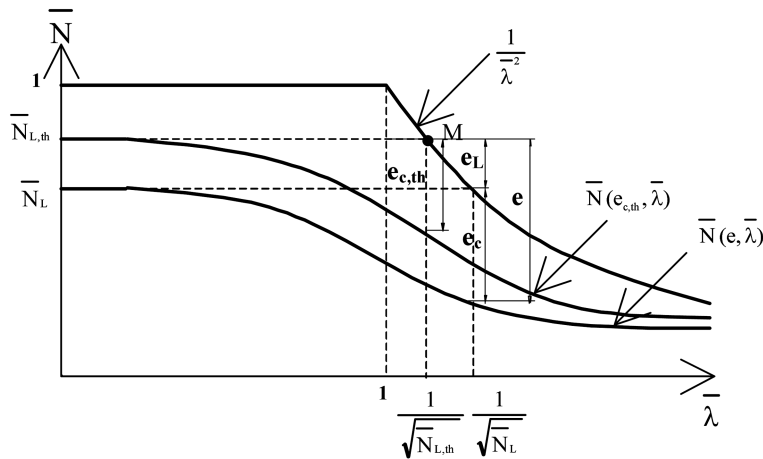


Fig. 6 The interactive buckling model based on the ECBL theory

The \bar{N} and \bar{M} values can be computed for perfect and imperfect shapes of both cross-section and member. Therefore, the erosion can be evaluated for different imperfection cases. If no imperfections, the evidence of interactive buckling effect only will be observed.

Further, the values of α (α_{LT}) imperfection sensitivity factor used in European buckling curves have been evaluated for all these imperfection shapes.

Table 5 “ α ” imperfection sensitivity factor for members in compression

Plain channel 96×36×1.5				
Imperfection mode	$\bar{N}_{L,th}$	\bar{N}_u	α	Buckling curve
PL1	0.551	0.101	0.322	b
PL2	0.551	0.109	0.304	b
PD1	0.549	0.207	0.155	a
PD2	0.549	0.204	0.158	a
PD3	0.549	0.083	0.354	c
PD4	0.549	0.078	0.365	c
PD5	0.549	0.248	0.113	a ₀
Lipped channel 96×36×12×1.5				
Imperfection mode	$\bar{N}_{L,th}$	\bar{N}_u	α	Buckling curve
LL1	0.633	0.347	0.109	a ₀
LL2	0.633	0.350	0.105	a ₀
LD1	0.655	0.281	0.215	b
LD2	0.655	0.371	0.109	a ₀
LD3	0.655	0.163	0.461	c
LD4	0.655	0.251	0.265	b
LD5	0.655	0.263	0.244	b

For the bar buckling modes the flexural imperfection of $L/1000$ and lateral-torsional imperfections given by Eq. (13) and Eq. (14) have been used.

The results of this analysis are summarised in Tables 5 and 6. In these tables $\bar{N}_{L,th}$ and $\bar{M}_{L,th}$ are the dimensionless (e.g. normalized with full sectional plastic strength) sectional strengths of members in compression and bending respectively; \bar{N}_u and \bar{M}_u are the dimensionless ultimate buckling strengths of

Table 6 “ α_{LT} ” imperfection sensitivity factor for members in bending

Plain channel 96x36x1.5				
Imperfection mode	$\bar{M}_{L,th}$	\bar{M}_u	α_{LT}	Buckling curve
PD1	0.518	0.207	0.140	a
PD2	0.518	0.214	0.132	a
PD3	0.518	0.213	0.134	a
PD4	0.518	0.208	0.137	a
PD5	0.518	0.211	0.137	a
PD6	0.518	0.206	0.142	a
Lipped channel 96x36x12x1.5				
Imperfection mode	$\bar{M}_{L,th}$	\bar{M}_u	α_{LT}	Buckling curve
LD1	0.886	0.532	0.292	b
LD2	0.886	0.539	0.277	b
LD3	0.886	0.545	0.267	b
LD4	0.886	0.522	0.310	b
LD5	0.886	0.490	0.391	c
LD6	0.886	0.476	0.422	c

slender members in compression and bending, respectively.

The values of α factor prove the higher sensitivity of distortional-overall interactive buckling to sectional imperfections. This fact can be explained by the lower post-critical strength reserve of distortional mode if compared with the local one.

Recently, based on a refined non-linear simulation with a GBT (e.g. General Beam Theory) model, a similar conclusion was drawn by Silvestre and Camotim (2004). The authors rigorously demonstrate the pure distortional imperfection shapes are the most detrimental ones, since they correspond to the lowest column strength. They also shown in case of members in bending the influence of local-sectional imperfection is low, while the initial unfavourable twist, combined with initial deflection, can significantly affect the ultimate strength.

4. Residual stresses

Residual stresses in cold-formed steel sections are due to cold-forming manufacturing process as well as to coiling and uncoiling of steel strips.

4.1. Membrane and flexural residual stresses

Adequate computational modelling of residual stresses is troublesome for the analysis. Inclusion of residual stresses (at the integration points of the model for instance) may be complicated. Selecting an appropriate magnitude is made difficult by a lack of data. As a result, residual stresses are often excluded altogether, or the stress-strain behaviour of the material is modified to approximate the effect of residual stresses.

In hot-rolled steel members residual stresses do not vary markedly through the thickness, which means the membrane residual stresses are dominant, while in cold-formed steel members residual stresses are dominant by a “flexural”, or through thickness variation. This variation of residual stresses may lead to early yielding on the faces of cold-formed steel plates and can influence their local buckling strength.

Residual stresses can be idealised as a summation of two types: flexural (FRSs) and membrane (MRSs) (see Fig. 7).

Experimental evidence shows more complex actual distributions of residual stresses. Fig. 8 presents the distribution of measured residual stress for a cold-formed steel lipped channel section (Rondal *et al.* 1994), while Fig. 9 provides evidence for residual flower for plain and lipped channel sections (Ungureanu 2003, Szabo 2004, Bivolaru 1993).

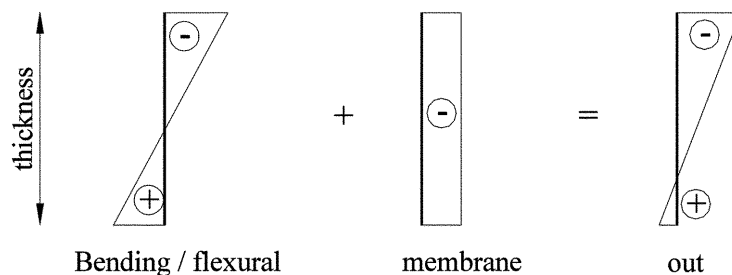


Fig. 7 Idealisation of residual stresses (Schafer and Peköz 1998)

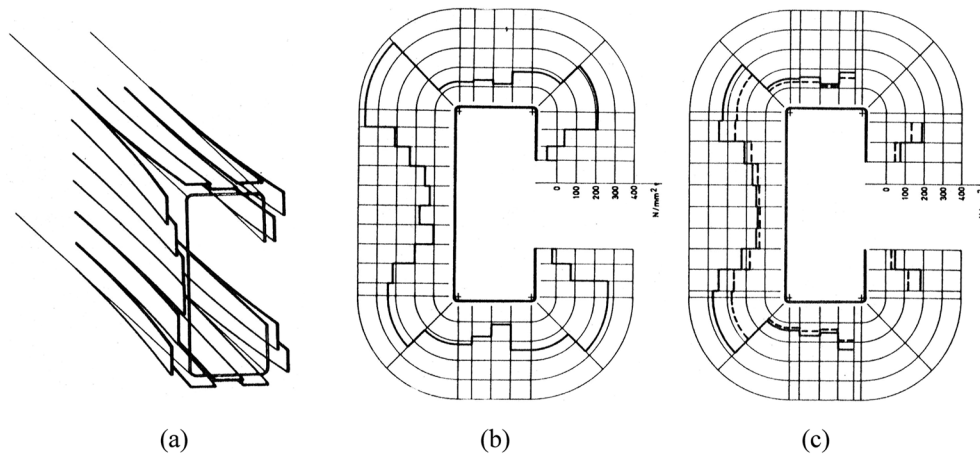


Fig. 8 Measurement of residual stresses in a cold rolled C profile:
(a) Residual “flower”; (b) Slicing method; (c) Curvature method (Rondal *et al.* 1994)

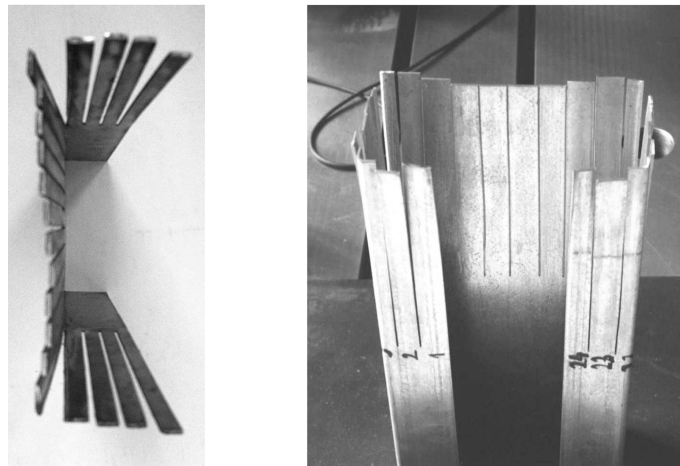


Fig. 9 Residual flower for plain channel and lipped channel sections

4.2. Codification of residual stresses

Schafer and Peköz (1998) collected and processed the statistically measured values for both membrane and flexural residual stresses. The results of their analysis are shown in Tables 7 and 8, expressed in percentage of yield strength of basic material.

However, some commentaries about the results of Tables 7 and 8 are necessary (Schafer and Peköz 1998), i.e.,

Membrane residual stresses. MRSs are more prevalent in roll-formed members than press-braked. Membrane residual stresses cause a direct lose in compressive strength. Significant MRSs exist primarily in corner regions. Opposing this effect, the yield stress (f_y) is elevated in corner regions due to significant cold work of forming. If large MRSs are modelled in the corners or other heavily worked

Table 7 Membrane residual stresses as ($\%f_y$)

Element	Roll-formed		Press-braked	
	Mean	Variance	Mean	Variance
Corners	6,8	1,1	5,2	0,4
Edge stiffened	3,9	1,0	0,9	1,0
Lip	7,9	1,5	0,2	0,3
Stiffened	-1,7	1,2	0,9	0,1

Table 8. Flexural residual stresses as ($\%f_y$)

Element	Roll-formed		Press-braked	
	Mean	Variance	Mean	Variance
Corners	26,8	5,0	32,7	3,3
Edge stiffened	23,5	1,0	8,0	2,5
Lip	6,7	6,4	56,0*	11,6
Stiffened	38,9	6,2	16,9	4,5

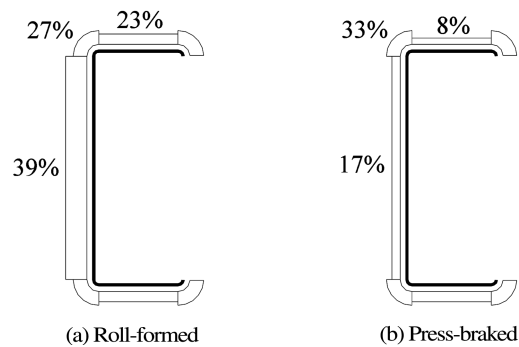
*Some lips are flame-cut, thus distorting this value.

zones, then increased yield stress in these regions should be modelled as well. Conversely, if MRSs are ignored, the elevation of the yield stress should not be included. More study is needed to show how much these two effects counteract one another.

Flexural residual stresses. FRSs are much more significant in cold-formed steel sections than MRSs ones. For member buckling (overall modes) the influence of FRSs is of lower importance, if compared with MRSs. However, local buckling can be significantly influenced by FRSs. Large magnitude flexural residual stresses in cold-formed sections are regularly observed - residual stresses equal to $50\%f_y$ are not uncommon. Measured FRSs also show a large degree of variation.

For the purpose of numerical analysis, Schafer and Peköz (1998) proposed the following approximate and conservative average distribution of flexural residual stresses (see Fig. 10).

Ungureanu (2003) used the curvature method (Rondal 1992) to evaluate the residual stresses for plain channels and “omega” sections obtained by press braking and suggested the following codification for flexural residual stresses (see Fig. 11). *Hat* section is in fact similar to a lipped channel.

Fig. 10 Average flexural residual stress as ($\%f_y$)

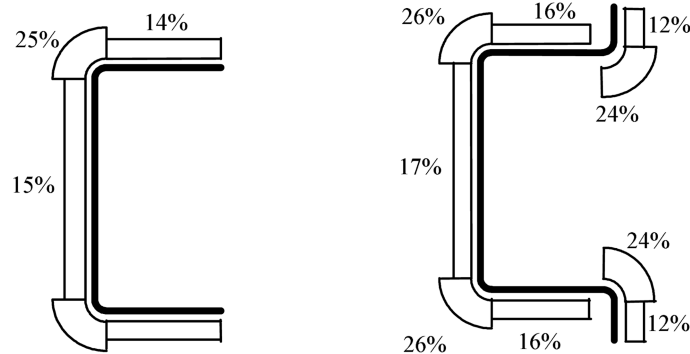


Fig. 11 Average flexural residual stress as ($\% f_y$) for plain channels and “omega” sections

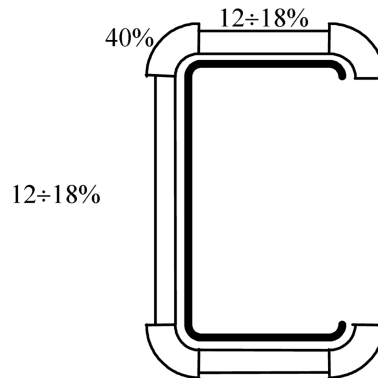


Fig. 12 Average flexural residual stress for a lipped channel as ($\% f_y$) proposed by Abdel-Rahman and Sivakumaran (1997)

To compare this codification, the one suggested by Abdel-Rahman and Sivakumaran (1997), which is shown in Fig. 12, can be considered, too.

Therefore, flexural residual stresses can influence the local buckling mode which could start earlier. The overall modes can be influenced by the membrane stresses (these is the case of hot rolled sections), but they are small in case of cold-formed sections.

The increase of yield strength at the corners is around (60-80)% and is of contrary sign compared to residual stresses. This means, when ultimate strength of the member is evaluated, considering the actual strength of the corners and the effective area of the walls, the effect of increased yield strength could be really stronger than residual stresses.

Particular cases are SHS and RHS sections, obtained by cold-forming, longitudinally welded. Gardner and Nethercot (2001) proposed a residual stress distribution to be used for numerical modelling of cold-formed stainless steel with such a type of section. According to their proposal, only the membrane stress introduced through welding needs to be explicitly defined in a finite element model. Gardner and Nethercot (2004) have shown that the effect of the residual stresses causes a small reduction in stiffness of the analysed stub and long columns but heaving little influence on their overall behaviour or ultimate load carrying capacities.

Table 9 Influence of flexural residual stresses on the ultimate load

Specimen	h (mm)		b (mm)	c (mm)		t (mm)	L (mm)	
UC8S1/1	151.1		99.5	-		1.98	360	
HC9S1/1	147.6		79.90	24.60		1.98	360	
Specimen	N_{exp} (kN)	N_{FEM1} (kN)	N_{FEM2} (kN)	N_{FEM3} (kN)	N_{FEM4} (kN)	N_{FEM5} (kN)	N_{FEM6} (kN)	
UC8S1/1	77.95	92.94	76.95	76.77	80.20	79.95	79.87	
HC9S1/1	119.6	130.5	116.0	116.3	122.3	121.7	121.67	

Rasmussen and Hancock (1993) observed that the tension and compression coupons cut from finished tubes curved longitudinally as a result of the through-thickness bending residual stresses. However, straightening of the coupons as part of the testing procedure approximately reintroduces the flexural residual stresses. Therefore, provided that the material properties of the cross-section are established from coupons cut from within the section, the effects of flexural residual stresses will be inherently present, and do not have to be explicitly defined in the finite element model (Gardner and Nethercot 2001).

The authors of this paper observed a similar situation in the case of thin-walled cold-formed members. Based on experimental research (Ungureanu 2003), and using the codification proposal of residual stresses, also sustained by Yiu and Peköz (2001), the behaviour of thin-walled cold-formed members was numerically simulated with and without the presence of residual stresses. The results obtained for plain channels and *hat* sections obtained by press braking are presented in Table 9.

where:

- N_{FEM1} – ultimate load obtained with no initial imperfections, no flexural residual stresses and the yield strength of the material cut from flat zones, $f_y = 228.61 \text{ N/mm}^2$;
- N_{FEM2} – ultimate load obtained with initial imperfections, no flexural residual stresses and the yield strength cut from flat zones, $f_y = 228.61 \text{ N/mm}^2$;
- N_{FEM3} – ultimate load obtained with initial imperfections, flexural residual stresses (codification from Fig. 11) and the yield strength cut from flat zones, $f_y = 228.61 \text{ N/mm}^2$;
- N_{FEM4} – ultimate load obtained with initial imperfections, no flexural residual stresses and the average yield (Eq. 7), $f_{ya} = 240.98 \text{ N/mm}^2$;
- N_{FEM5} – ultimate load obtained with initial imperfections, flexural residual stresses (codification from Fig. 11) and the average yield strength (Eq. 7), $f_{ya} = 240.98 \text{ N/mm}^2$;
- N_{FEM6} – ultimate load obtained with initial imperfections, flexural residual stresses (codification from Fig. 11), increased two times, and the average yield strength (Eq. 7), $f_{ya} = 240.98 \text{ N/mm}^2$.

It can be observed there is no significant influence of flexural residual stresses as Gardner and Nethercot (2004) have shown.

5. Conclusions

1. If test results are available, the input parameters for material model are needed to describe the stress-strain behaviour directly obtained from tensile coupon tests from different portions of the member cross-section, including the corner properties. If test results are not available, an idealisation of the material model, which is elastic-plastic with strain hardening, can be conveniently approximated by

Ramberg-Osgood or Powell equations. Using ANSYS, the ideally elastic-plastic material model can be implemented by means of bilinear isotropic plastic model (BISO), and Ramberg-Osgood model by means of multi-linear model (MISO). One can see that both characteristic values and shape of load-deflection curves do not differ significantly for the two models. In what concerns the influence of the increase of yield strength at the corners of a given section on its ultimate strength, a crucial point is the ratio between the corner areas and the total area of that cross-section. A larger bent radius generates a larger area of the corners. Some authors (Karren and Winter 1967, Abdel-Rahman and Sivakumaran 1997) recommend to include in the “corner area” some adjacent parts from the flat walls. More increase the “corner area” larger is the increase of ultimate strength of the section (Ashraf *et al.* 2004). However, for thin-walled cold-formed steel members obtained by press-braking, with small bent radius, the role of corner properties is negligible (Szabo 2004). For the case when sections with small corner radii are modelled, the corner properties do not need to be introduced explicitly into the model, while for bigger corner radii, the shape and afferent properties must be introduced in numerical model. Also, the analyst has to take into account the fabrication technology of modelled member (cold rolling or press braking process).

2. In a two-mode interacting buckling (e.g. local-overall interaction) different shapes of local-sectional imperfections have different effects on the ultimate strength of the member. The higher sensitivity of the distortional-overall interactive buckling to sectional imperfections is generally confirmed. This can be explained by the lower post-critical strength reserve of the distortional mode, compared with the local one. Therefore, this is understandable, because the local buckling strength formula is based on the plate buckling model, characterised by a stable bifurcation and a higher post-critical reserve compared with the bar bifurcation, which is used in the calculation model of distortion. Thus, the appropriate identification and selection of imperfection shape and size associated to the relevant instability mode are crucial for analysis.

3. In thin-walled cold-formed steel members the residual stresses induced by cold-forming are predominantly of flexural type, while the membrane stresses are negligible. Inclusion of residual stresses in numerical analysis is generally complicate because selection of their appropriate magnitude is difficult by the lack of systematic data. However, numerical studies performed by the authors of this paper and other researchers showed that there is no significant influence of flexural residual stresses on the ultimate strength of the sections. Moreover, Rasmussen and Hancock (1993) observed that the tension and compression coupons cut from finished tubes curved longitudinally as a result of the through-thickness bending residual stresses. However, straightening of the coupons as part of the testing procedure approximately reintroduces the flexural residual stresses. Therefore, when the material properties of the cross-section are established from coupons cut from within the section, the effect of flexural residual stresses is inherently present, and no need to be explicitly defined in the finite element model (Gardner and Nethercot 2001).

4. Therefore, for thin-walled cold-formed steel sections, the effect of geometrical imperfections is significantly greater than residual stresses and the change of yield strength. Consequently, special care has to be paid to geometrical imperfections and, among them, accounting for the actual performance of fabrication technology, the sectional imperfections are the most important.

5. However, if a good practice guide is intended to be produced for numerical simulations, as a basis of further design codes in this matter, supplementary research is necessary in order to identify and codify the critical imperfection modes, accounting for forming process, material properties, technology and the shape of cross-sections.

References

- Abdel-Rahman, N. and Sivakumaran, K.S. (1997), "Material properties models for analysis of cold-formed steel members", *J. Struct. Eng.*, ASCE, **123**(9), 1135-1143.
- Ashraf, M., Gardner, L. and Nethercot, D.A. (2004), "Numerical modelling of the static response of stainless steel sections", *Proc. Int. Colloquium Recent Advances and New Trends in Structural Design*, 7-8 May 2004, Timisoara, Romania, 1-10.
- AS 4100-1990, Australian Standard: Steel Structures, Homebush, Australia, 1990.
- Bakker, M.C.M. and Pekoz, T. (2003), "The finite element method for thin-walled members – Basic principles", *Thin Walled Structures*, **41**(2-3), 179-190.
- Batista, E.M. (1986), "Essais de profils C et U en acier plies a froid", Laboratoire de Stabilité des Constructions. Université de Liege, Rapport Nr. 157, Septembre 1986.
- Bernard, E.S., Coleman, R. and Bridge, R.Q. (1999), "Measurement and assessment of imperfections in thin-walled panels", *Thin Walled Structures*, **33**, 103-126.
- Bivolaru, D. (1993), "Numerical methods and technical experimentation in determination of residual stresses in cold-formed profiles", Diploma work, University of Liege.
- Bjorhovde, R. (1972), "Deterministic and probabilistic approaches to the strength of steel columns", PhD Dissertation, Lehigh University, PA.
- Dubina, D., Goia, D., Zaharia, R. and Ungureanu, V. (1997), "Numerical modelling of instability phenomena of thin-walled steel members", *Proc. of 5th Int. Colloquium on Stability and Ductility of Steel Structures - SDSS'97*, Nagoya, Japan, 29-31 July 1997, **2**, 755-762.
- Dubina, D. (2000), "Recent research advances and trends on coupled instabilities of bar members, General Report", *Coupled Instabilities in Metal Structures-CIMS'2000*, Imperial College Press, London, 131-144.
- Dubina, D. and Ungureanu, V. (2002), "Effect of imperfections on numerical simulation on instability behaviour of cold-formed steel members", *Thin Walled Structures*, **40**(3), 239-262.
- Dubina, D. (2001), "The ECBL approach for interactive buckling of thin-walled steel members", *Steel and Composite Structures*, **1**(1), 75-96.
- E.C.C.S.: European Recommendations for the Design of Light Gauge Steel Members, ECCS, Brussels, 1978.
- EN 1993-1-3 EUROCODE 3, Design of Steel Structures, Part 1.3: General Rules, Supplementary Rules for Cold-Formed Thin-Gauge Members and Sheeting, CEN/TC 250/SC3–European Committee for Standardisation, Brussels, 2001.
- Gardner, L. and Nethercot, D.A. (2001), "Behaviour of cold-formed stainless steel cross-sections", *Proc. of 9th Nordic Steel Construction Conf. – NSCC2001*, Helsinki, Finland, 18-20 June, 781-789.
- Gardner, L. and Nethercot, D.A. (2004), "Numerical modeling of stainless steel structural components – A consistent approach", *J. Struct. Eng.*, ASCE, **130**(10), 1586-1601.
- Karren, K.W. (1967), "Corner properties of cold-formed steel shapes", *J. Struct. Div.*, ASCE, **93**, ST1.
- Karren, K.W. and Winter, G. (1967), "Effects of cold-forming on light-gage steel members", *J. Struct. Div.*, ASCE, **93**, ST1.
- Put, B.M., Pi, Y.-L. and Trahair, N.S. (1998), "Lateral buckling tests on cold-formed channels beams", Research Report No. 767, University of Sydney, April 1998.
- Rasmussen, K.J. and Hancock, G.J. (1988), "Geometric imperfections in plated structures subject to interaction between buckling modes", *Thin Walled Structures*, **6**, 433-452.
- Rasmussen, K.J. (1996), "General report on numerical simulation and computational models", *Coupled Instabilities in Metal Structures – CISM'96*, Imperial College Press, London, 45-60.
- Rondal, J. (1992), "Détermination théorique des contraintes résiduelles dans les éléments en acier profilés à froid". Ce travail a reçu le prix N.V. BEKAERT S.A. 1992, octroyé par le Fonds National de la Recherche Scientifique.
- Rondal, J., Dubina, D. and Bivolaru, D. (1994), "Residual stresses and the behaviour of cold-formed steel structures", *Proc. of 17th Czech and Slovak Int. Conf. on Steel Structures and Bridges*, Bratislava, Slovakia, September 7-9, 193-197.
- Rondal, J. (2005), "Peculiar problems in cold-formed steel design. Part 2", in *Light Gauge Metal Structures - Recent Advances*, CIMS Courses and Lectures No. 455, Ed. by J. Rondal and D. Dubina, Springer Wien New

- York, 16-22.
- Rondal, J. and Dubina, D. (2003), "Computational modelling and analysis of cold-formed steel members", *Proc. of Steel Structures and Bridges 2003, The 20th Czech and Slovak Nat. Conf.* - Prague, Czech Republic, 535-540.
- Rondal, J., Dubina, D. and Ungureanu V. (2004), "Imperfections and computational modelling of cold-formed steel members", *Proc. of Int. Colloquium Recent Advances and New Trends in Structural Design*, 7-8 May 2004, Timisoara, Romania, 209-220.
- Schafer, B.W. and Peköz, T. (1998), "Computational modelling of cold-formed steel characterising geometric imperfections and residual stresses", *J. Constructional Steel Research*, **47**, 193-210.
- Schafer, B.W., Grigoriu, M. and Peköz, T. (1998), "A probabilistic examination of the ultimate strength of cold-formed steel elements", *Thin Walled Structures*, **31**, 271-288.
- Silvestre, N. and Camotim, D. (2004), "GBT-based analysis of the local-plate/distortional buckling mode interaction in lipped channel columns", *Proc. of the 4th Coupled Instabilities in Metal Structures – CIMS'04*, 27-29 September 2004, Rome, Italy, 107-118.
- Sridharan, S. (2000), "General report on numerical simulation and computational models for coupled instabilities", *Coupled Instabilities in Metal Structures – CISM'2000*, Imperial College Press, London, 61-72.
- Szabo, I. (2004), "Study of constructional systems and structural performances of steel frames for storage racks", PhD Thesis, The "Politehnica" University of Timisoara, Romania.
- Ungureanu, V. (2003), "Lateral-torsional buckling of thin-walled cold-formed beams", PhD Thesis, The "Politehnica" University of Timisoara, Romania.
- Yiu, F. and Peköz, T. (2001), "Design of cold-formed steel plain channels", Research Report, Cornell University, Ithaca, USA.